CONF-9509149--16

LA-UR-96-175

BEAM LOSSES AND BEAM HALO IN ACCELERATORS FOR NEW ENERGY SOURCES

RECEIVED
MAR 13 1996
OSTI

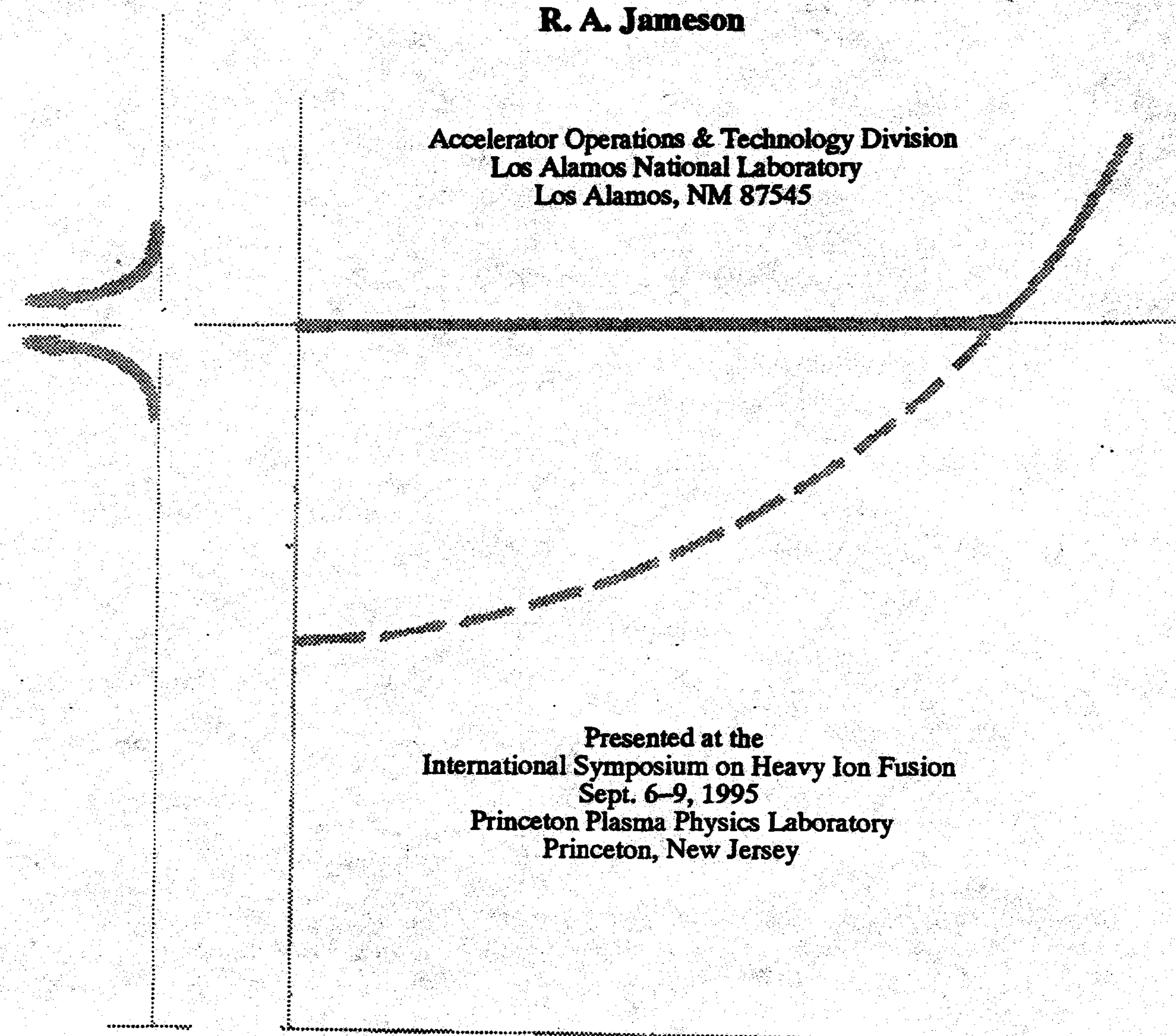

R. A. Jameson

Accelerator Operations & Technology Division
Los Alamos National Laboratory
Los Alamos, NM 87545

Presented at the
International Symposium on Heavy Ion Fusion
Sept. 6–9, 1995
Princeton Plasma Physics Laboratory
Princeton, New Jersey

Work performed under the auspices of the US Department of Energy. The support and hospitality of the Alexander von Humboldt Stiftung, the Institut für Angewandte Physik of the University of Frankfurt, and the Japan Atomic Energy Research Institute are gratefully acknowledged.

NOTICE

Page(s) size did not permit electronic reproduction. Information may be purchased by the general public from the National Technical Information Service, U.S. Department of Commerce, Springfield, VA 22161 (Area Code 703-487-4650). DOE and DOE contractors may purchase information by contacting DOE's Office of Scientific and Technical Information, P.O. Box 62, Oak Ridge, TN 37831, Attn: Information Services (Area Code 423-576-8401).

Beam Losses and Beam Halos in Accelerators for New Energy Sources

R.A. Jameson
AOT-1 MS H817
Los Alamos National Laboratory
Los Alamos, NM 87545
rjameson@lanl.gov

Abstract

Large particle accelerators are proposed as drivers for new ways to produce electricity from nuclear fusion and fission reactions. The accelerators must be designed to deliver large particle beam currents to a target facility with very little beam spill along the accelerator itself, in order that accelerator maintenance can be accomplished without remote manipulators. Typically, particle loss is preceded by the formation of a tenuous halo of particles around the central beam core, caused by beam dynamics effects, often coupled with the slight imperfections inevitable in a practical design. If the halo becomes large enough, particles may be scraped off along the accelerator. The tolerance for beam spill in different applications is discussed, halo mechanisms and recent work to explore and understand their dynamics are reviewed, and possible directions for future investigation are outlined.

1. Consequences of Halos - Beam Losses

Prevention of stray beam losses is necessary in both light and heavy ion machines, for somewhat different reasons.

Light ions, such as protons and deuterons, have long stopping ranges, penetrate deeply, and have nuclear reactions that cause radioactivity buildup in the linac structure. This radioactivation is the main problem with beam losses in light ion machines. It is desired to be able to maintain the machine without using remote manipulators ("hands-on" maintenance) over the life of the facility, usually estimated at 40 years. The beam loss rule-of -thumb is $\leq$ 1 nA/m/GeV, or with a 100 mA beam, $\leq 1\times10^{-8}$ beam spill per meter at 1 GeV. This radioactivity requirement is much more severe than a specification on beam loss that would cause heating or damage problems, even for superconducting structures. The main mechanism that causes beam losses in light-ion machines is space-charge beam dynamics in vacuum. Direct Coulomb collisions and background gas scattering are small effects or negligible. A new concern in cw machines may be neutralization effects with ion-electron instabilities [1].

Heavy ions have short stopping range and deposit all their energy very near the surface. The main problem with lost beam is heating. Estimates [2] are that 1×10^{-3} of a HIF driver beam at one spot would cause instantaneous melting, and that $\leq 1\times10^{-5}$ should be maintained to prevent undesired heating in a room-temperature structure. Detailed estimates have not been made for superconducting structures, but are probably of order 1×10^{-8}. Radioactivation is less of a problem, though still significant. Neutron production estimates [3] in present HIF driver designs are 4x typical LAMPF performance; it is assumed that improvements could lower this to 2x LAMPF for > 100 MeV. This would allow hands-on maintenance, but it would be desirable to reduce the losses further. The main loss mechanisms are stripping and background gas scattering, followed by space-charge beam dynamics.

2. Prevention of Halos and Beam Losses

The primary goal of the author's studies is to prevent beam losses by proper design. Investigation of beam halos that lead to losses is of secondary importance, however fascinating, except as it leads to the necessary understanding to prevent them. It is clear that a completely uniform, or linear, system would not have beam losses; it does not exhibit spurious beam size evolution or emittance growth; it does not have free energy that can be converted into these effects. Prevention of halos involves control of nonlinearities in both external and space-charge fields, instabilities, and particularly, resonances. Halos can form when this control is not complete, and free energy is available. Detailed energy balance (complete equipartitioning, or nonlinear matching - not just equipartitioning to prevent excitation of instabilities) is thus desired and forms the logical basis for a design philosophy. From this basis, which may not be completely achievable in practice, the consequences can be assessed.

Detailed equipartitioning clearly means that the beam must be at least rms matched everywhere, and detailed nonlinear local matching is desired. This means that the machine, in terms of its space-charge physics (characterized by tunes, tune depressions, etc.) must be smooth, with smooth transitions between stages. A minimum of knobs is desired, and also an insensitivity of beam-loss performance to beam current, because tuning must be done from small current up to the full operating current. Present linac designs are now empirically tending toward this practice; by proper consideration of the space-charge parameters at transitions, the tunes are kept smooth and complex matching sections external to the linac structures are eliminated. Beam halo and both total and rms emittance growth are still typically observed, however, as indicated in Figs. 1 and 2 for a long proton linac and an 8 MeV RFQ, in which both the accelerating gradient and the zero-current transverse phase advance per unit length were held constant.

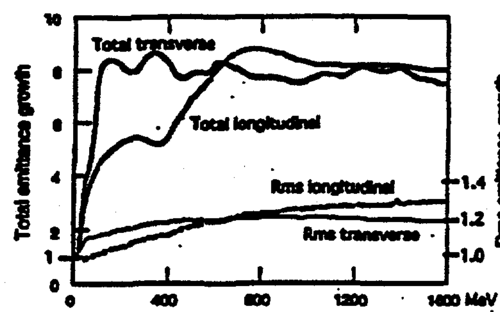

Fig. 1. Beam size and emittance behavior in a 1 GeV proton rf linac, with constant accelerating gradient and $\sigma_0{}^t$ per unit length.

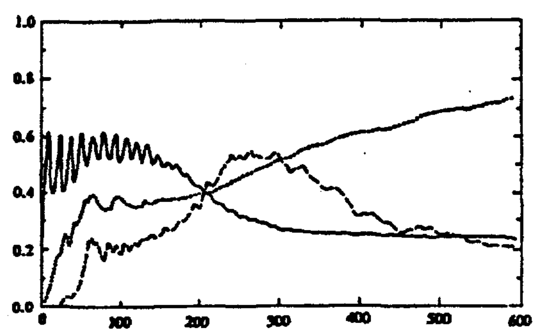

Fig. 2. Emittance behavior and rms equipartitioning ratio in an 8 MeV RFQ, with constant $\sigma_0{}^t$ per unit length from the shaper end (~cell 50) to the output, and constant ϕ_s from the gentle buncher end (~cell 250) to the output. Transverse (solid) and longitudinal (dotted) normalized rms emittance, mm·mrad; equipartitioning ratio (dashed). Only the transmitted particles are used for the emittance and tune computations.

The rms equipartitioning ratio [4] $(eln \cdot \sigma^l)/(etn \cdot \sigma^t) = 1$ when the beam is equipartitioned between transverse and longitudinal phase-spaces, where eln and etn are the normalized transverse and longitudinal rms emittances and σ^t and σ^l are the phase advances with beam. In Fig. 2 we see the beam is not equipartitioned. In the following, work to improve the emittance performance is discussed.

3. The Hofmann Chart of Tune Space

3.1 Coherent Instabilities

Hofmann [5] has used a tune-space chart (Fig. 3) to portray the instability thresholds of various coherent space-charge modes of the KV distribution in a 2-degree-of-freedom focusing channel. It was found [5,6] that the thresholds are also quite accurate for non-KV beams in a focusing channel, and for r-z ellipsoidal warm-beam distributions in channels with and without acceleration.

A point on the chart requires that the ratio of emittances in the two degrees of freedom be defined as >1; the larger emittance defines the variable x. Plotting the tune trajectory [6] of an actual linac design on the chart is done using the emittance ratio, which may be changing, at each point, and the local phase advances. The thresholds are functions of the emittance ratio. When the trajectory falls under a threshold, emittance exchange between the degrees of freedom can be expected. The rate of exchange cannot be predicted with certainty analytically, but has been estimated [7] for different categories of unbalance; if triggered, it typically is quite fast, on the order of a few plasma periods before an equipartitioned equilibrium is reached. Numerical work has indicated that the equipartitioning ratio can vary from unity by as much as ~1.5:1 before the incoherent

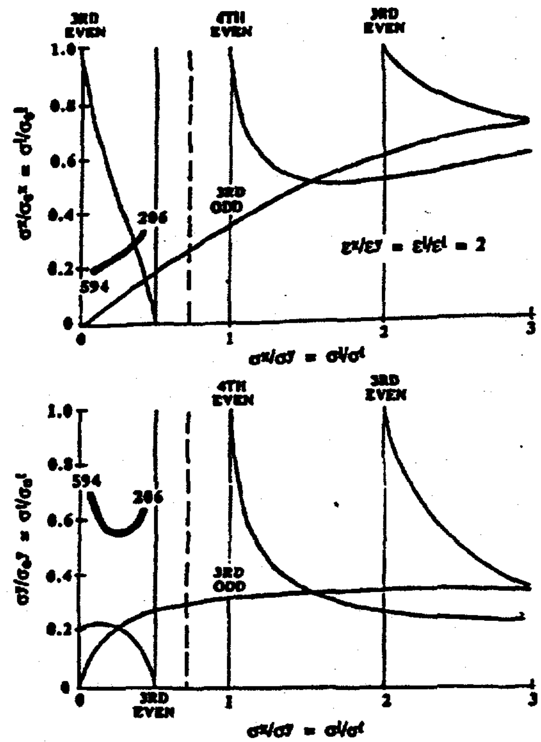

Fig. 3. The Hofmann Chart for eln/etn = 2, showing thresholds for 3rd-odd, 3rd-even and 4th-even coherent instability modes for the 2-D KV distribution. The tune trajectory from cell 206 (end of the shaper) to the output at cell 594 for the RFQ of Fig. 2 is plotted on the chart. The vertical line at $\sigma^l/\sigma^t = 0.5$ is the equipartitioned condition for eln/etn = 2. The line at $\sigma^l/\sigma^t = 1/\mathrm{Sqrt}[2]$ maintains this σ^l/σ^t at any beam current.

instability is triggered. Equipartitioning via these coherent space-charge mode instabilities can properly be described in terms of a "thermalization" of the beam, that may tend toward a Maxwell-Boltzman equilibrium [8], but more probably, toward a 'quasi-stationary" distribution, characterized as an equilibrium determined by the underlying channel dynamics and not by thermalization in the sense of randomization or diffusion.

In earlier linacs and RFQs [6], part of the trajectory typically fell below one or more thresholds and equipartitioning from this effect was a contributor to emittance growth. The exchange was usually masked by other effects that caused observations to show emittance growth in both planes.

Contemporary rf linac design, such as the RFQ of Figs. 2 and 3 has evolved empirically to usually avoid the unstable regions. The RFQ as a buncher has largely enabled this by affording a much smaller longitudinal to transverse rms emittance ratio than was possible with the older double-drift buncher systems. The trajectory of the 1 GeV linac of Fig. 1 also avoids the instability regions. Thus while the tune trajectory of any proposed design should always be checked relative to these lowest-order collective space-charge modes, a typical "good" rf linac design can avoid them.

This means that the emittance growth of concern in Figs. 1 and 2 apparently does not come from these modes, and we have to search further for the mechanism. Note [9] that there is an equipartitioning action occurring in the Fig. 2 RFQ in the region of cells 150-594; with increase in the longitudinal rms emittance, and decrease in the transverse. The question of whether this action could be caused by higher-order collective instabilities was discussed with I. Hofmann [5], who has simulated higher modes also, but found they had little effect. We are led to suggest that the emittance behavior in Figs. 1,2 and 4 is fed instead by higher-order single-particle modes, as discussed below.

3.2 Equipartitioned Trajectory

When the beam is equipartitioned, eln/etn = $\gamma b/a = \sigma^t/\sigma^l$, where a and b are the transverse and longitudinal radii of the beam, and γ is the relativistic gamma. Thus for a given emittance ratio, $\sigma l/\sigma t$ is fixed (Fig. 3), and an equipartitioned trajectory with no emittance change would remain on this vertical line. Previous [6] and on-going numerical work is geared to exploring linac designs with this property. We have demonstrated [9] that an RFQ acceleration section designed for an equipartitioned beam can result in evolution of the dc injected beam to an equipartitioned beam at the output (Figs. 4 & 5). The RFQ design trajectory was set analytically for equipartitioning at eln/etn = 2 (thus σ^l/σ^t = 1/2) from the end of the shaper to the output.

Work in subsequent linac stages is aimed at enforcing an equipartitioned tune trajectory using the external fields and actual beam self-

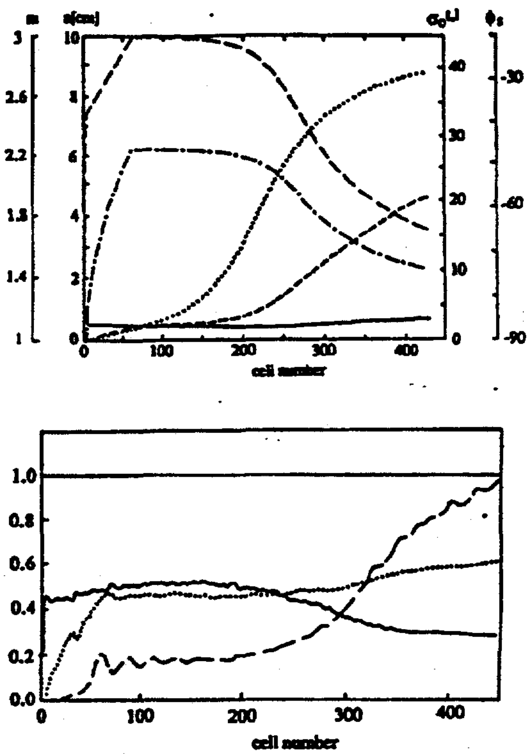

Fig. 4. a) Design curves, b) emittance behavior, and c) Hofmann Chart of an RFQ designed as an equipartitioned channel with eln/etn = 2 from the end of the shaper to the output. The longitudinal tune is fixed by maintaining the vane voltage at a given Kilpatrick factor; the transverse tune is then set to give equipartition at the design current.

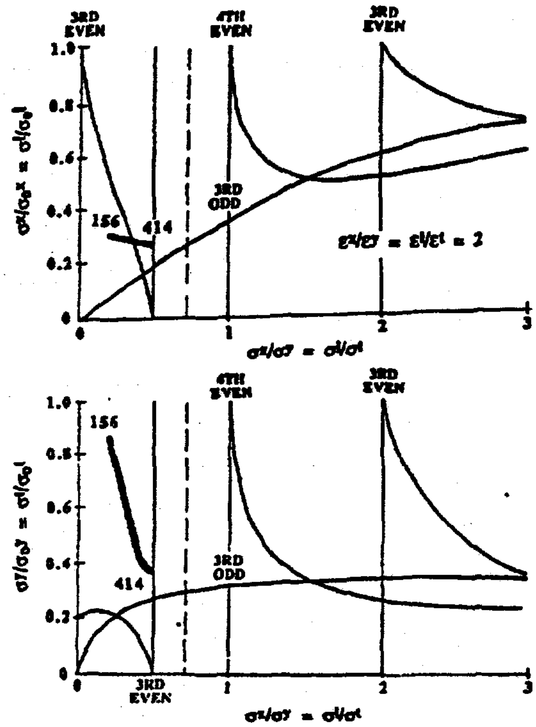

Fig. 5. For the RFQ of Fig. 4, the actual beam evolves approximately to the design condition at the output.

consistently [4]. We wish to combine this strategy with roles that resonances play in emittance growth, discussed below, to see if careful equipartitioning can minimize beam size and emittance growth.

3.3 Zero Sensitivity of σl/σt to Beam Current

The nonlinear beam envelope and equipartitioning equations demonstrate many fascinating features [10] still under investigation. For example, there is a tune ratio given by $(\sigma^t/\sigma^l)^2 = 2\,ff / (1 - ff)$, where ff is the ellipsoidal bunch form factor ~ $a/3\gamma b$, that, for a given emittance ratio, is not a function of beam current. Fig. 3 indicates this line, at $\sigma^l/\sigma^t \approx 1/\mathrm{Sqrt}[2]$ for eln/etn = 2.

This is a very useful design guide, because tune-up and operation of practical machines require operation over the full range of beam current and insensitivity of the tuning to current is valued. The underlying connection between this line and the equipartitioned line is being investigated.

4. Single Particle Modes

We make use of the tune chart of Fig. 6 for this discussion. Space-charge causes a realistic warm distribution to have a tune spread. Defining the tune in successive rings of charge [11] produces a curve like the upper, with the tune on axis being the rms tune depression found in the envelope and equipartitioning equations. An alternative, very useful, definition [12] assigns an instantaneous phase advance to each particle based on the net external vs. space-charge forces on the particle. This phase advance

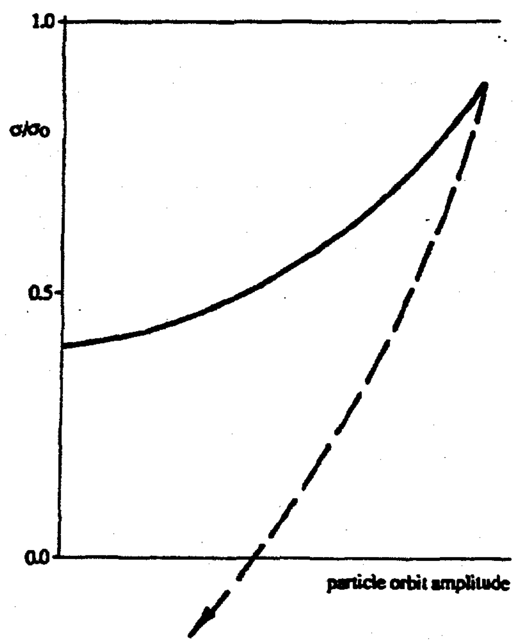

Fig. 6. Tune depression vs. particle orbit amplitude. Solid curve results from using rings of charge to characterize the particle distribution; dashed curve results from definition of a single particle instantaneous phase advance.

can be strongly negative (space-charge repulsion can stop a particle, and send it backwards). Thus the effective tune-spread in an intense rf linac bunch can be very large.

A non-equilibrium condition, which can be described as a lack of exact local matching, has free energy available that is available by different mechanisms to drive the beam distribution toward an equilibrium. One mechanism is the collective modes discussed above. In a periodic external focusing system, resonances play a key role in the particle dynamics. Here we want to discuss the interplay between space-charge and resonance influences on particle tunes, using three examples. The key point is that once a particle enters the resonance band, the resonance will tend to trap the particle tune to the resonant tune, unless another force successfully competes to prevent the trapping, or help the particle escape.

4.1 Mismatch

In a continuous, periodic radial focusing channel, an equilibrium distribution derived from the system Hamiltonian can be constructed that has a tune spread similar to that of Fig. 6. Mismatching the radius of the initial distribution will cause the beam envelope, and the density of the beam core, to oscillate at a breathing mode frequency. The single-particle tunes oscillate as indicated in Fig. 7. It has been carefully shown [12,13] that some particles will undergo a three-step process that causes them to move out of the core into a diffuse halo.

The first action is that if a particle passes through the core of the beam as the central density is rising, a large amount of energy can be transferred to the particle, and it will attain a larger radius after leaving the core. (Conversely, if passing through as the core density is decreasing, it can lose energy to the core and come out at a smaller radius.)

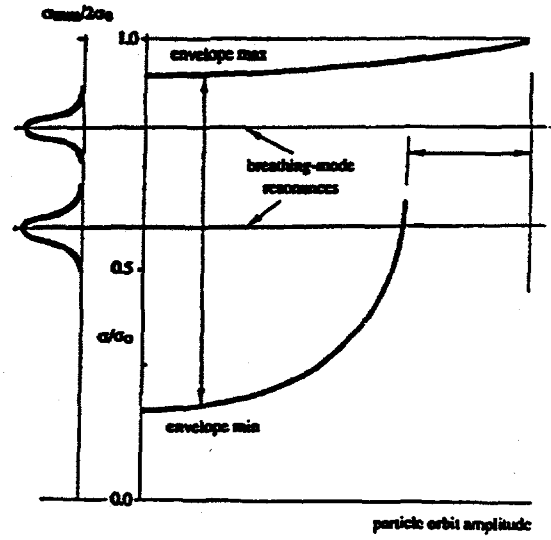

Fig. 7. Tune depression excursion for a radially mismatched beam.

Second, in a periodic system, if the same particle crosses the core on the next oscillation when again the core density is rising, the radius increase will be resonantly enhanced.

Third, since the particle tune increases with radius as indicated in Fig. 7, its orbit frequency will change, and eventually it will fall out of resonance, typically beginning to cross the core as the density is falling and moving back into the core.

Beam halo from this mechanism is formed from a continuing exchange of particles in and out of the halo.

Utilizing the instantaneous particle phase-advance definition, the population can be precisely identified and the statistics determined.

A very important point is that the actual dynamics of such mechanisms must be studied using self-consistent simulations. The test-particle methods most often used give much useful information, but are not solutions to the actual problem.

Using data from a self-consistent simulation, Fig. 8 shows the detailed radial motion of a particle that migrates between the beam core and a halo. The behavior can be completely described in terms of the modern chaos literature of the standard map. The particle first escapes the core and moves strongly out into the halo at about step 9000. It stays outside awhile, but its tune changes, it falls behind on the main mismatch resonance, and goes back into the core at about step 15000. The process repeats. It is seen that the particle begins to be attracted toward the main mismatch resonance early in the run, but works its way slowly to the escape. In the meantime, the particle gets caught in a succession of weaker rational number resonances (the island chains). It stays caught in one of these resonance, for example of period eight, until the attraction of the main resonance and the chance space-charge interactions as it traverses the beam distribution result in its escape (turnstile out) from that resonance and its entrapment in one of a longer period - moving always closer to the separatrix that characterizes the main resonance. Finally, the main mismatch

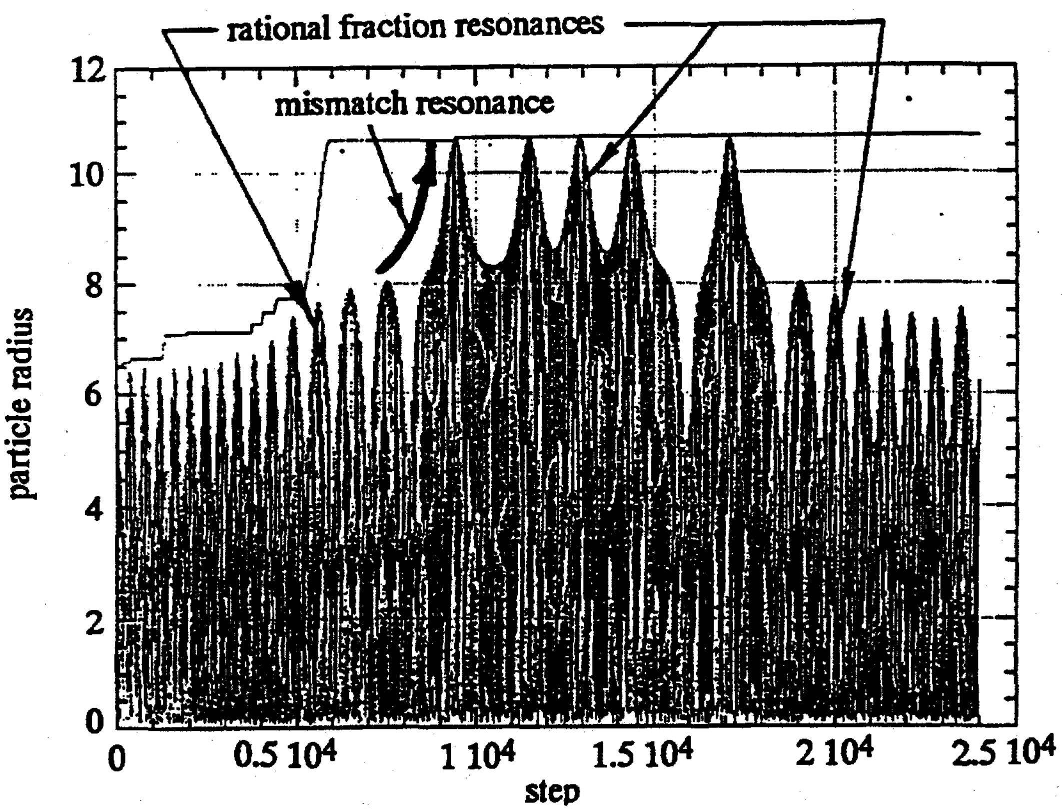

Fig. 8. Mismatched Hamiltonian initial distribution in a continuous, linear focusing channel, with space-charge factor = 0.54 and mismatch = 1.30. Solid line is maximum radius of all particles. Oscillating line is the detailed radius of the particle that achieved the maximum radius during the run, showing that the dynamics involves many rational fraction resonances as well as the main mismatch resonance.

resonance wins and the particle is swept out into the halo, actually crossing the separatrix (on which it would have an infinite period and could continue out forever; it does not get caught exactly because the particle tune changes with orbit amplitude). It oscillates outside on similar resonances, again being drawn back toward the separatrix, which it jumps across again as it goes back in, etc. Resonances of quite high order are involved in Fig. 8 — the island chain nearest the escape across the mismatch separatrix is of order 20.

There is a quite definite threshold for the beginning of halo formation from this type of mismatch, as a function of the degree of mismatch and amount of space-charge, and also a strong self-limiting of the halo amplitude at about 1.5 times the radius expected from the degree of mismatch. The fraction of particles migrating to and from the halo increases as space-charge increases. The threshold indicates that mismatch should be kept below 15-20%. The competition between space-charge and resonance forces accounts for these effects. The mismatch causes the tune distribution to sweep back and forth; thus particles are driven across the breathing mode resonance and until the resonance becomes strong enough (sufficient mismatch), it cannot dominate. Because the particle tune changes with orbit radius, it will interact both in-phase and later out-of-phase with the resonance and its outward movement is self-limiting. As space-charge increases, the tune-shift in the beam core flattens as the core distribution becomes more uniform, so more particles are in unison in their interaction with the resonance.

4.2 Ring Half-Integer Resonance

This example dramatically shows how an extremely strong resonance can completely dominate the dynamics. The discussion is taken directly from Machida's excellent paper [11]. Fig. 9 indicates a very strong resonance at some tune. Consider the

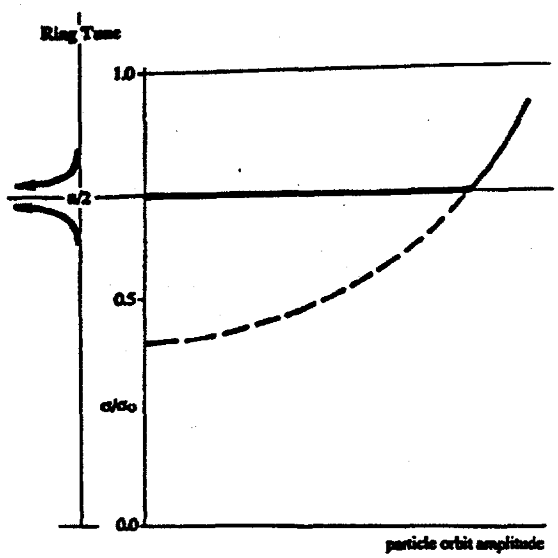

Fig. 9. Tune depression diagram for a system with a very strong resonance.

situation where it is attempted to create a beam distribution with a space-charge tune spread as in Fig. 6, by increasing the beam current from zero. The tune will begin to spread, but as particle tunes enter the strong resonance bandwidth, they are trapped and cannot escape. As Machida states, the resonance *causes* a channel intensity limit. If one insists on raising the current farther, trying to reach a stronger tune depression, something has to give to maintain consistency - the beam emittance would grow so the channel can carry more current at the constrained tune. Machida finds that high-order single particle resonances are the mechanism by which the emittance grows. As would be expected, the resonances with largest effect are those reflecting the underlying periodicity of the machine lattice. He is able to verify this by specific use of test-particle probes.

This example is one of many where circular machine studies have long probed situations that are of relevance to high-intensity linac designers, making it clear that one should become completely cognizant of this literature. As indicated above, the literature of chaos is also fully descriptive, and so is the literature of plasmas. It is a matter of finding the right translation for linacs, where different effects (collective, single-particle, etc.) occur with similar time scales so it is hard to separate them and arrive at design rules.

4.3 High-Order Single-Particle Modes in RMS Matched High-Intensity RF Linacs

We can now return to the mechanism of the emittance and equipartitioning behavior observed in Figs. 1 – 5. The rf linac depends on alternating-gradient transverse focusing, and this lattice will determine the strongest features of the system resonances. The strong envelope resonance at $\sigma_o{}^t = 90°$ is always avoided by choosing $\sigma_o{}^t < 90°$. Higher-order resonances (5x72°, 6x60°, 8x45°, 12x30°, etc.) cannot be totally avoided in practice. Longitudinal motion in the linac brings in other tunes, there are couplings between longitudinal and transverse, and various types of nonlinearities. Many rational fraction combinations are possible, as indicated in the mismatch case, Fig. 8. As indicated in Fig. 10, the individual strength of these resonances may be small, but the combination of them can affect the single-particle dynamics to the extent that even the core of the beam may experience emittance growth. It is hypothesized here that these single-particle modes are the mechanism sought to explain the growth and equipartitioning still observed in some linac designs that are basically smooth and rms matched, as exemplified above. This then defines a systematic direction for intended future work to identify the operational modes in actual conditions, especially with acceleration, which introduces new features into the dynamics. The type of equipartitioning occurring in this case might also be properly described as a "thermalization", but self-consistent work is needed to determine the type of equilibrium distribution, probably a 'quasi-stationary' one.

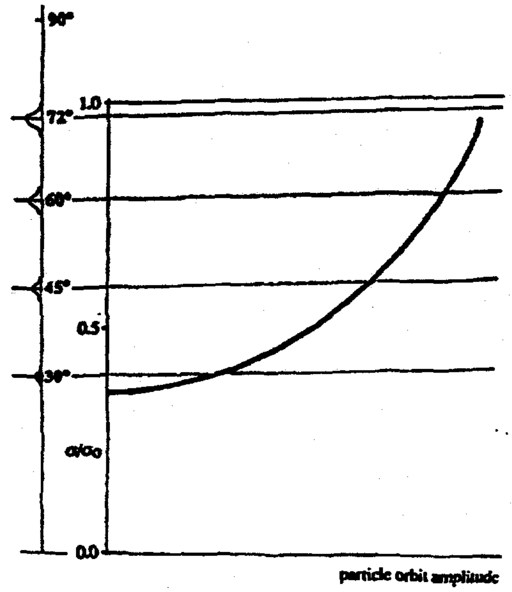

Fig. 10. Tune depression diagram for a system with lattice and rational number resonances.

Work with the KV distribution [14] in transport channels indicated that $\sigma_o{}^t$ should be chosen <60° to avoid instability. Parallel simulations with a full rf linac and realistic beam distributions [6] indicated that the situation may not be so restrictive, and one might be able to aim for the $\sigma_o{}^t$, around 80°, that gives the smallest average transverse beam size (but high flutter factor). Lagniel [15] has recently explored two-dimensional focusing without acceleration using test-particle methods, and concludes that σ_0^t should be kept below 60° and σ_0^l below ~20°. The true situation must be explored self-consistently, however, as all the possibilities mapped with test-particles may not be actually accessed, some interesting features, such as the chaotic bands, may not be the most important, and the test-particle methods do not allow the halo formation thresholds and statistics to be measured.

5. Three Dimensions and Symmetries

The breathing mismatch modes studied above [12,13] were simulated using a ring model for space-charge. I. Hofmann [16] pointed out a key issue. The ring-model is appropriate in the case studied because it has the same symmetry as the mode being studied.

The strong tune dependence with orbit amplitude causes the strong self-limiting observed for the mismatch mode. In the one-dimensional studies, this self-limiting is absolute, and particles could never migrate to infinite amplitude from this mismatch effect (there are KAM curves beyond the separatrix, and these cannot be penetrated). It is probably true that surfaces analogous to KAM curves exist for this type of action in more degrees of freedom also, although this is not provable because higher-dimensional phase-spaces are not separable into two parts. I wonder if such a proof would be possible if the appropriate symmetry limitations were built into the proof? In this case, it might be possible to discuss the boundary of the action and relate that to the desired machine design rule or tolerance, without need to know more about the internal details. This is another important avenue of inquiry for the appropriate modes.

However, Hofmann also pointed out that the orbit amplitude tune dependence, and thus the strong self-limiting observed in the mismatch modes, may not hold for all effects that may be present. In circular machines, there are modes in which the tune is not amplitude dependent, and thus paths on which a particle could travel to infinity without tune change. P. Channell [17] has indicated that misalignment in a linac has this property, and has described the appropriate separatrix. This is no doubt the reason that the author had difficulty understanding misalignment results in the ring-model simulation – the space-charge subroutine symmetry was wrong. It is clear that care must be taken to be sure the symmetry in the simulation is correct for the problem at hand, and this unfortunately means that full 3-D routines, taking much more computer time, are really necessary for realistic and self-consistent work.

Acknowledgments

Extended interactions with I. Hofmann and Machida's paper [11] were instrumental in greatly clarifying my present view and approach to the questions of collective vs. single-particle and resonance effects. The support of the Alexander von Humboldt-Stiftung and the US DOE, and the hospitality of H. Klein and the Institut für Angewandte Physik at the University of Frankfurt are gratefully acknowledged.

References

[1] P. Channell, private communication.

[2] P. Strehl, GSI Workshop on Heavy Ion Fusion, August 1995.

[3] FEAC7 1993 Report

[4] R.A. Jameson, Beam-intensity limitations in linear accelerators, IEEE Trans. Nucl. Sci. 28, p. 2408, June 1981.

[5] I. Hofmann, Emittance growth of beams close to the space charge limit, IEEE Trans. Nucl. Sci. 28, No. 3, 2399, June 1981.

[6] R.A. Jameson, Equipartitioning in linear accelerators, Proc. of the 1981 Linear Accelerator Conf., Santa Fe, NM, October 19-23, 1981, Los Alamos National Laboratory Report LA-9234-C, p. 125, February 1982.

[7] F.W. Guy and T.P Wangler, Numerical studies of emittance exchange in 2-D charged particle beams, 1986 Linear Acc. Conf. Proc., 336, SLAC-303, Sept 1986.

[8] N. Brown and M. Reiser, Thermal equilibrium of bunched charged particle beams, Phys. Plasmas 2 (3), 965, March 1995.

[9] D. Li and R.A. Jameson, Equipartitioning and emittance growth in RFQ linacs, submitted to N.I.M. A, Nov. 1995.

[10] R.A. Jameson, On scaling & optimization of high intensity, low-beam-loss RF linacs for neutron source drivers, AIP Conf. Proc. 279, ISBN 1-56396-191-1, DOE Conf-9206193 (1992) 969-998.

[11] S. Machida, Space-charge effects in low-energy proton synchrotrons, N.I.M., A (1991)43-59.

[12] R.A. Jameson, Self-consistent beam halo studies & halo diagnostic development in a continuous linear focusing channel, LA-UR-94-3753, Los Alamos National Laboratory, 9 November 1994. To be published in AIP Proceedings of the 1994 US-CERN-Japan Topical Course on Accelerator Physics & Technology, Maui, Hawaii, November 1994.

[13] R.A. Jameson, Beam-halo from collective core/single-particle interactions, LA-UR-93-1209, Los Alamos National Laboratory, March 1993, and R.A. Jameson, Design for low beam loss in accelerators for intense neutron source applications - The physics of beam halos", 1993 Particle Accelerator Conference, Washington, D.C., 17-20 May 1993, IEEE Conference Proceedings, IEEE Cat. No. 93CH3279-7, 88-647453, ISBN 0-7803-1203-1.

[14] I. Hofmann, L.J. Laslett, L. Smith and I. Haber, Particle Accelerators 13, 145 (1983).

[15] J.M. Lagniel, Chaotic behaviour and halo formation from 2-D space-charge dominated beams, N.I.M. A 345, 1994.

[16] I. Hofmann, private communications.

[17] P. Channell, private communication.